

## Orientation of microfibrils and microtubules in developing tension-wood fibres of Japanese ash (*Fraxinus mandshurica* var. *japonica*)

A.K.M.A. Prodhon, R. Funada, J. Ohtani, H. Abe, K. Fukazawa

Laboratory of Wood Biology, Department of Forest Science, Faculty of Agriculture, Hokkaido University, Sapporo 060, Japan

Received: 1 September 1994 / Accepted: 6 October 1994

**Abstract.** The orientation of cellulose microfibrils (MFs) and the arrangement of cortical microtubules (MTs) in the developing tension-wood fibres of Japanese ash (*Fraxinus mandshurica* Rupr. var. *japonica* Maxim.) trees were investigated by electron and immunofluorescence microscopy. The MFs were deposited at an angle of about 45° to the longitudinal axis of the fibre in an S-helical orientation at the initiation of secondary wall thickening. The MFs changed their orientation progressively, with clockwise rotation (viewed from the lumen side), from the S-helix until they were oriented approximately parallel to the fibre axis. This configuration can be considered as a semi-helicoidal pattern. With arresting of rotation, a thick gelatinous (G-) layer was developed as a result of the repeated deposition of parallel MFs with a consistent texture. Two types of gelatinous fibre were identified on the basis of the orientation of MFs at the later stage of G-layer deposition. Microfibrils of type 1 were oriented parallel to the fibre axis; MFs of type 2 were laid down with counterclockwise rotation. The counterclockwise rotation of MFs was associated with a variation in the angle of MFs with respect to the fibre axis that ranged from 5° to 25° with a Z-helical orientation among the fibres. The MFs showed a high degree of parallelism at all stages of deposition during G-layer formation. No MFs with an S-helical orientation were observed in the G-layer. Based on these results, a model for the orientation and deposition of MFs in the secondary wall of tension-wood fibres with an S<sub>1</sub> + G type of wall organization is proposed. The MT arrays changed progressively, with clockwise rotation (viewed from the lumen side), from an angle of about 35–40° in a Z-helical orientation to an angle of approximately 0° (parallel) to the fibre axis during G-layer formation. The parallelism between MTs and MFs was evident. The density of MTs in the developing tension-wood fibres

during formation of the G-layer was about 17–18 per µm of wall. It appears that MTs with a high density play a significant role in regulating the orientation of nascent MFs in the secondary walls of wood fibres. It also appears that the high degree of parallelism among MFs is closely related to the parallelism of MTs that are present at a high density.

**Key words:** Cellulose microfibril – Cortical microtubule – *Fraxinus* – Gelatinous layer – Tension-wood fibre

### Introduction

Woody plants develop fibres or tracheids with a highly organized wall architecture. The secondary walls of these wood fibres and tracheids have a three-layered (S<sub>1</sub>, S<sub>2</sub> and S<sub>3</sub> layers from outside to inside) structure with intermediate layers (for review, see Harada and Côté 1985). This multilayered structure is due to a shift in the angle of MFs relative to the longitudinal axis of the fibre (Harada et al. 1958; Dunning 1968, 1969). The concept of a helicoidal pattern or a twisted pattern, composed of a series of planes in which the direction of MFs changes progressively, has been proposed for the plant cell wall (for reviews, see Neville and Levy 1984, 1985; Roland et al. 1987). In the secondary walls of wood fibres and tracheids, a similar structure and rotative changes in the orientation of depositing (innermost) MFs have been observed (for reviews, see Parameswaran and Liese 1982; Roland and Mosiniak 1983; Satiat-Jeunemaitre 1986; Abe et al. 1991; Kataoka et al. 1992), supporting the validity of such a concept. However, the reported details of the microfibrillar organization in the secondary wall are not in full agreement from study to study. Roland and Mosiniak (1983) and Abe et al. (1991) suggested that MFs are deposited successively in one direction with changes in their speed of rotation; when rotation is arrested, a thick wall layer with a consistent texture is deposited. By contrast, Kataoka et al. (1992) found repeated alternation in the direction of rotation

---

Abbreviations: FE-SEM = field emission scanning electron microscopy; G = gelatinous layer; MF = cellulose microfibril; MT = cortical microtubule; S<sub>1</sub> = outermost layer of the secondary wall; TEM = transmission electron microscopy

Correspondence to: R. Funada; FAX: 81 (11) 736 1791

during deposition of MFs, which caused a thick secondary wall. Such differences of opinion in relation to the thickening of the secondary wall in fibres or tracheids remain to be resolved.

Investigations on the mechanism of MF deposition reported in the literature indicate that the orientation of MTs is parallel to the orientation of newly deposited MFs. In addition, MT-depolymerizing agents usually disrupt the orientation of nascent MFs. Thus, most of the published studies support the hypothesis that MTs play an important role in controlling the orientation of MFs, as proposed initially by Ledbetter and Porter (1963). A number of investigations relating to this hypothesis have been performed with a variety of cell walls of lower and higher plants (for reviews, see Hepler and Palevitz 1974; Palevitz and Hepler 1976; Gunning and Hardham 1982; Mueller and Brown 1982; Giddings and Staehelin 1991; Seagull 1992, and references therein). Similar parallelism between MFs and MTs has infrequently been described in the case of the secondary walls of developing wood fibres or tracheids in woody plants (for reviews, see Cronshaw 1965; Hirakawa 1984; Inomata et al. 1992; Abe et al. 1994). However, the precise role of MTs in the regulation of the orientation of MFs remains to be determined because several exceptions have been reported (for reviews, see Neville and Levy 1985; Emons et al. 1992, and references therein). Therefore, more detailed examinations of the co-alignment of MTs and MFs are needed.

In the present investigation, we examined the changes in orientation of MFs and MTs in the developing tension-wood fibres of Japanese ash (*Fraxinus mandshurica* Rupr. var. *japonica* Maxim.) trees which we have observed to have an S<sub>1</sub> + G type of wall organization (data not shown). Tension-wood is usually characterized by the presence of gelatinous fibres, which form a G-layer. It is considered that this layer is composed entirely or almost entirely of MFs with a high degree of both crystallinity (Norberg and Meier 1966) and parallelism, and the MFs are oriented parallel or nearly parallel to the longitudinal axis of the fibres (for reviews, see Côté and Day 1965; Mia 1968; Côté et al. 1969; Scurfield 1973). Thus, it seems that tension-wood is a suitable material for a detailed investigation of the organization of MFs. However, information on tension-wood in this regard is very limited (Nobuchi and Fujita 1972; Robards and Kidwai 1972; Fujita et al. 1974). In the present study, we used field emission scanning electron microscopy (FE-SEM), which has the advantage of revealing the orientations of MFs and MTs at high resolution over relatively larger areas than can be visualized by transmission electron microscopy (TEM) (Abe et al. 1991, 1992, 1994). We did, however, also examine the orientation of MTs by immunofluorescence microscopy and TEM.

## Materials and methods

**Plant materials.** Samples of Japanese ash (*Fraxinus mandshurica* Rupr. var. *japonica* Maxim.) trees, grown on a plantation at Nakagawa Experimental Forest of Hokkaido University, were selected for this investigation. Several trees of about nine years of age and 3–4 m in height had been inclined artificially at an angle of 30°

to the vertical at the beginning of the initiation of cambial growth in the early spring. During the period of active growth, sample discs were collected from the leaning trees at breast height. Small blocks of tissues containing phloem, cambial zone, differentiating xylem and mature xylem were obtained from the upper sides (tension-wood) of the leaning tree trunks. The blocks were divided into small pieces, and adjoining pieces containing similar stages of differentiation were used for different microscopic observations.

**Field emission scanning electron microscopy (FE-SEM).** The plant materials were fixed in 3–4% glutaraldehyde (in 0.1 M phosphate buffer, pH 7.2) at room temperature for 5–6 h. For the observation of MFs, plant materials were plasmolysed in a 0.8 M solution of saccharose for 1 or 2 d at room temperature before fixation in glutaraldehyde. Then small blocks of about 8 mm (longitudinal direction) × 6 mm (radial) × 3 mm (tangential) were cut from the wood samples and washed in distilled water. The longitudinal radial surfaces that were to be examined were exposed with a freezing-sliding microtome. These samples were treated with a dilute solution of sodium hypochlorite for 1–5 min to remove cytoplasm. After a further wash with distilled water, the samples were post-fixed in 1% osmium tetroxide in the same buffer for 2 h at room temperature. After washing with buffer and with distilled water, the materials were dehydrated in a graded ethanol series and dried by the *t*-butyl alcohol freeze-drying method. For observations of MTs, the plant materials had been fixed directly in glutaraldehyde. The materials were washed with distilled water, post-fixed and then dehydrated in a similar manner to that described above. The samples were dried by the critical-point method and the longitudinal radial surfaces that were to be examined were exposed on a sliding microtome. Finally, all the dried materials were lightly coated with platinum or with platinum and carbon in a vacuum evaporator. The specimens were observed with an FE-SEM (S-800; Hitachi, Tokyo, Japan) at an accelerating voltage of 3–5 kV.

The density of MTs was taken as the number of MTs oriented perpendicular to a 1 µm unit length of wall of a developing tension-wood fibre. The measurements were made at about 50 places from at least 10 fibres in the region of developing tension-wood during formation of the G-layer. Enlarged FE-SEM micrographs were used for counting of MTs.

**Transmission electron microscopy (TEM).** The plant materials were fixed in 3–4% glutaraldehyde (in 0.1 M phosphate buffer, pH 7.2) at room temperature for 5–6 h and were cut into thin radial longitudinal pieces. They were post-fixed for 1 h in 1% osmium tetroxide in the same buffer. After washing with buffer and with distilled water, the samples were dehydrated in a graded ethanol series. Finally, the samples were embedded in araldite or epoxy resin. Some ultrathin sections were cut on an ultramicrotome (UltraCut J; Reichert, Vienna, Austria) with a diamond knife and were stained with uranyl acetate and then with lead citrate. Specimens were then observed with a transmission electron microscope (JEM-100C; JEOL, Tokyo, Japan) at an accelerating voltage of 100 kV. Enlarged TEM micrographs were also used for determinations of the density of MTs.

**Immunofluorescence microscopy.** Immunofluorescence microscopy was used for visualization of MTs. The specimens were treated by a modified version of the methods of Roberts et al. (1985), Iwata and Hogetsu (1988) and Kang et al. (1993) for immunofluorescent staining. They were fixed overnight at room temperature in a mixture of 3.6% paraformaldehyde plus 0.2% glutaraldehyde, that contained 10% dimethylsulfoxide (DMSO) and 0.1% Nonidet P-40 in 50 mM Pipes [piperazine-N,N'-bis(2-ethanesulfonic acid)] buffer (pH 7.0), supplemented with 5 mM ethylene glycol-bis(β-aminoethyl ether)-N,N,N',N'-tetraacetic acid (EGTA) and 5 mM MgSO<sub>4</sub>. After fixation, the blocks were frozen, without washing, in a drop of distilled water on a freezing stage and sectioned radially at a thickness of 15–30 µm with a sliding microtome. After three washes for 3 min each with PBS (phosphate-buffered saline: 137 mM NaCl, 2.7 mM KCl, 1.5 mM KH<sub>2</sub>PO<sub>4</sub>, 8.0 mM Na<sub>2</sub>HPO<sub>4</sub>, adjusted to pH 7.3), the sections were incubated with 30 µl of a solution of antibodies against

$\alpha$ -tubulin for 45 min at 25 °C. A mouse monoclonal antibody against chicken  $\alpha$ -tubulin was used at a dilution of 1:500 in PBSB (PBS containing 0.1% NaN<sub>3</sub> and 1 mg/ml bovine serum albumin). After three washes for 3 min each with PBS, the sections were incubated for 45 min at 25 °C with 30  $\mu$ l of a solution of fluorescein isothiocyanate (FITC)-conjugated antibodies that had been raised in sheep against mouse immunoglobulin G (IgG) and diluted 1:10 in PBSB. The incubations with all antibodies were performed on a sheet of Parafilm (American Can Co., Greenwich, Conn., USA). Antibodies used in this experiment were purchased from Amersham Japan Co. (Tokyo, Japan). The sections were washed three times with PBS and mounted on glass slides in 50% glycerol in PBS that had been supplemented with 0.1% *p*-phenylene diamine.

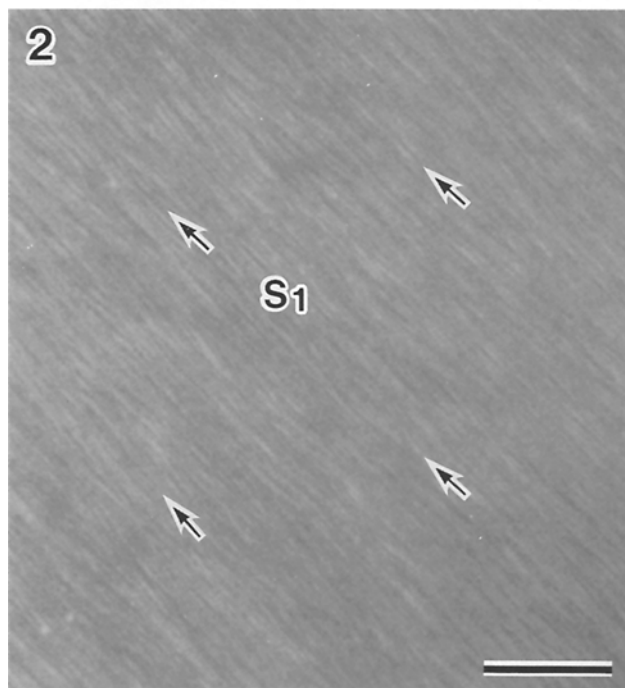
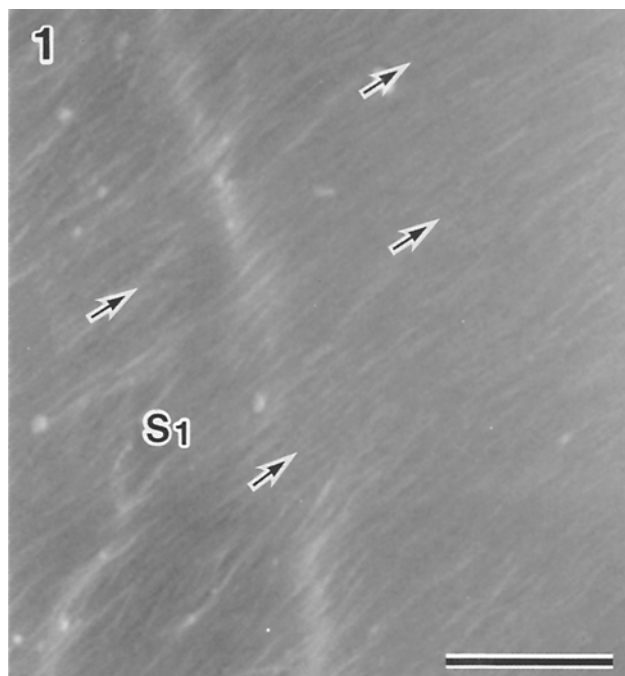
Observations were made under an epifluorescence microscope (Zeiss Co., Oberkochen, Germany) with a B-extraction system and an LP-520 barrier filter.

## Results

**Orientation of cellulose microfibrils.** Figures 1 through 8 show the orientation of MFs on the inner surfaces of developing tension-wood fibres in a radial file undergoing various stages of secondary wall deposition, as observed by FE-SEM. These developing fibres were observed successively from the cambium to mature fibres on the xylem side. Examination of such a series of fibres allowed observation of the successive changes of microfibrillar orientation within the same specimen. It should be noted that the helical direction of MFs as seen from the outside of the fibre wall is designated as S- or Z-helix relative to the longitudinal axis of the fibre; the direction of the oblique stroke in each letter being used to indicate the left-hand and right-hand inclination, respectively. In the present investigation, the helical direction of the microfibrillar orientation appears to be reversed, because we viewed samples from the lumen side.

Figure 1 shows the outermost layer (S<sub>1</sub>) of the secondary wall, in which MFs were ordered and deposited at an angle of about 45° to the longitudinal axis of the fibre in an S-helix. This profile corresponds to the initiation of secondary wall thickening. The MFs changed their orientation progressively with clockwise rotation, as viewed from the lumen side, and were deposited perpendicular to the fibre axis (micrograph not shown). Next, the orientation of MFs changed progressively with clockwise rotation and, MFs were deposited over the transversely oriented MFs in a Z-helix (Fig. 2). The stage at which the S<sub>1</sub> layer formed was restricted to three or four developing tension-wood fibres in a radial file.

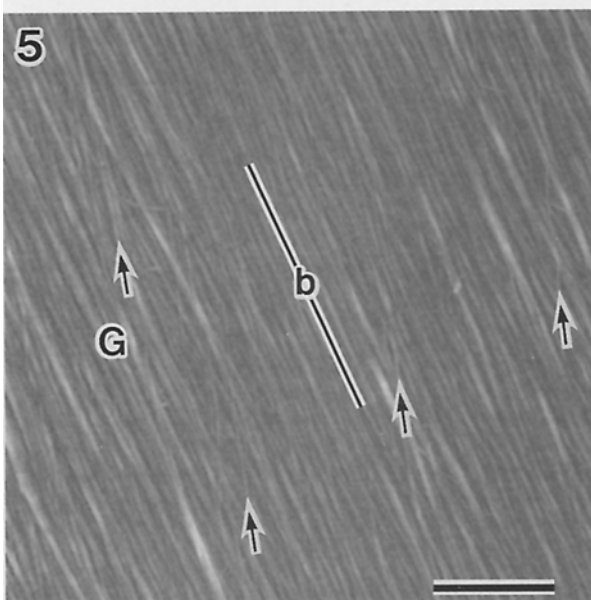
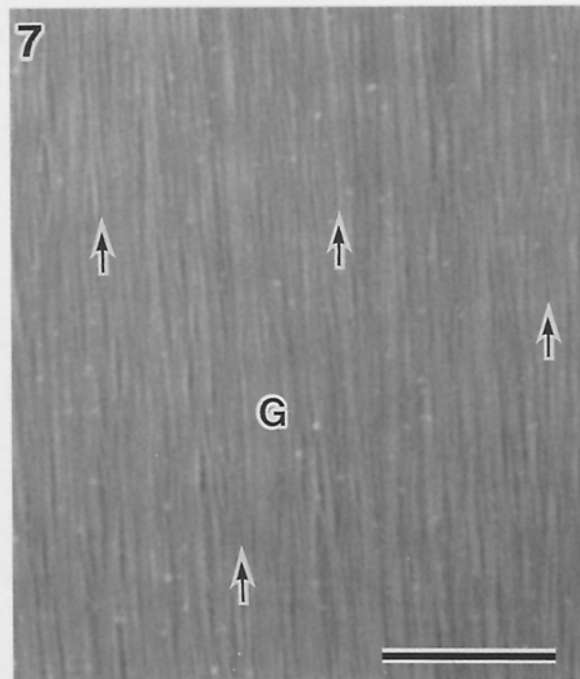
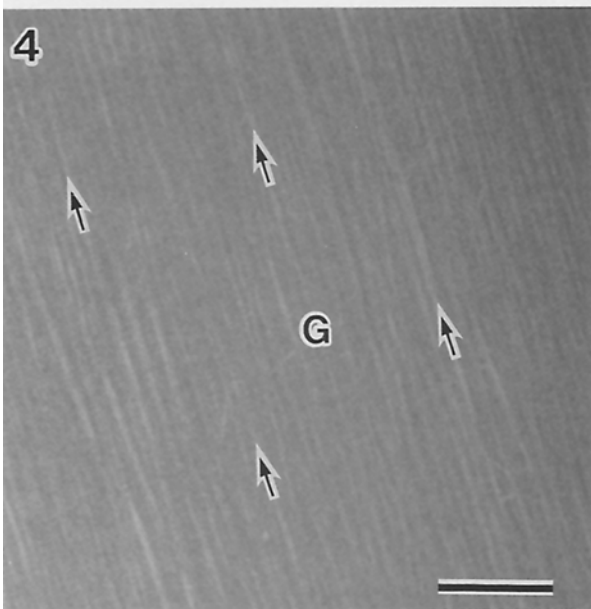
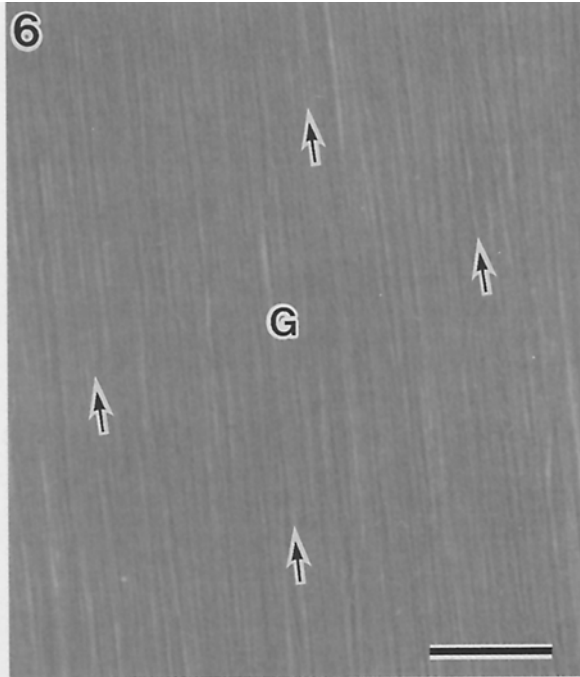
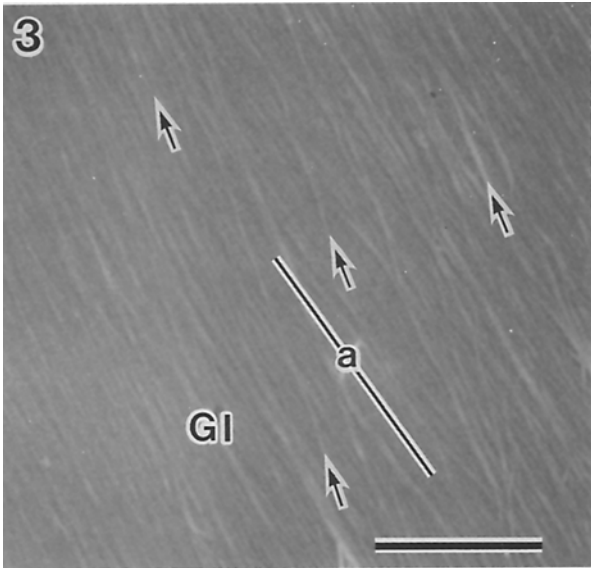
The shift of MFs occurred continuously in the same direction (with clockwise rotation) until MFs were oriented parallel (at an angle of approximately 0°) to the fibre axis (Figs. 3–7). Figure 3 shows that the newly laid down MFs (arrows) were oriented at an angle of about 30° to the fibre axis in a steep Z-helix over the MFs (a) that had been deposited previously at an angle of about 35–40° to the longitudinal axis of the fibre in a Z-helix. The orientation of MFs in Fig. 4 is similar to that of the newly laid down MFs in Fig. 3. The texture of newly deposited MFs (arrows) reveals a high degree of parallelism, suggesting the initiation of G-layer deposition. The MFs were closely spaced and evenly deposited. They were more or less compact in terms of texture and the underlying MFs



**Figs. 1, 2.** Micrographs (FE-SEM) showing the progressive changes in the orientation of MFs, with clockwise rotation, in the S<sub>1</sub> layer (viewed from the lumen side) of tension-wood fibres of Japanese ash **Fig. 1.** The MFs (arrows) in the S<sub>1</sub> layer, oriented at an angle of about 45° to the fibre long axis in an S-helix, at the initiation of secondary wall thickening. S<sub>1</sub>, outermost layer of the secondary wall. Bar = 0.5  $\mu$ m

**Fig. 2.** The orientation of MFs (arrows) in a Z-helix at a later stage of formation of the S<sub>1</sub> layer. S<sub>1</sub>, outermost layer of the secondary wall. Bar = 0.5  $\mu$ m

were not visible. In Figure 5, newly laid down MFs (arrows) were oriented at an angle of about 15° to the fibre axis in a steep Z-helix over the MFs (b) that had previously been deposited at an angle of about 30° to the fibre



axis in a steep Z-helix. Figure 6 shows that the newly deposited MFs (arrows) were oriented at an angle of about  $10^\circ$  to the fibre axis in a steep Z-helix. The MFs were closely spaced and evenly deposited with a high degree of parallelism and, therefore, the underlying MFs were invisible. Figure 7 shows that the newly laid down MFs (arrows) were oriented parallel to the fibre axis. The MFs were also located close to each other with a high degree of parallelism, and the underlying MFs were not visible because of the even deposition of the MFs. The MFs in Figures 6 and 7 were observed to be compactly arranged in terms of texture.

The deposition of MFs in the G-layer, parallel to the fibre axis, continued as a result of the arresting of rotation and, consequently, the G-layer became thickened with a consistent texture of parallel MFs. No MFs were observed in the G-layer with an S-helical orientation.

At a later stage of G-layer deposition, two types of gelatinous fibre were observed on the basis of the orientation of MFs on the innermost surfaces of gelatinous fibres. In the case of type 1, MFs were oriented parallel to the fibre axis (Fig. 7). In type 2, MFs changed their orientation with counterclockwise rotation from the orientation parallel to the fibre axis (Fig. 8). Figure 8 shows the counterclockwise rotation of newly deposited MFs (arrows) oriented at angles of about  $15\text{--}20^\circ$  to the fibre axis, in a steep Z-helix, over the MFs (c) that had been previously deposited parallel to the fibre axis. The counterclockwise rotation of MFs showed a variation in orientation, which ranged from an angle of  $5^\circ$  to an angle of  $25^\circ$  among the fibres. The counterclockwise rotation of MFs was less gradual than the clockwise rotation of MFs in the G-layer. The MFs in the G-layer showed a high degree of parallelism at all stages of deposition during formation of the G-layer.

**Orientation of cortical microtubules.** Field emission scanning electron micrographs, viewed from the lumen side, revealed the arrangement of MTs in the developing tension-wood fibre during formation of the G-layer (Figs. 9–11). At the early stage of G-layer formation, the MTs were oriented at an angle of about  $35\text{--}40^\circ$  to the longitudinal axis of the fibre with a Z-helical orientation (Fig. 9). Thereafter, the orientation of MTs changed progressively, with clockwise rotation (viewed from the lumen side), until the MTs were oriented parallel to the fibre axis (Figs. 9–11). Figure 10 shows that MTs were arrayed at an angle of about  $10^\circ$  to the fibre axis with a steep Z-helical ori-

entation. In Figure 11, the MTs are oriented parallel to the longitudinal axis of the fibre. This pattern of progressive changes in orientation of MTs was similar to that of MFs in the G-layer, illustrated in Figs. 4–7. We could not observe the counterclockwise rotation of MTs at the end of G-layer deposition or the MTs during formation of the  $S_1$  layer because damage to specimens was severe, and the cytoplasm had become detached from cell walls.

The density of MTs in the developing tension-wood fibres during formation of the G-layer was about  $17\text{--}18$  per  $\mu\text{m}$  of wall. The MTs were close to each other and there was a high degree of parallelism between them.

Immunofluorescence micrographs revealed that the bundle-like aggregates of MTs were arrayed obliquely, parallel or nearly parallel to the fibre axis in the developing tension-wood fibres during formation of the G-layer (Figs. 12, 13).

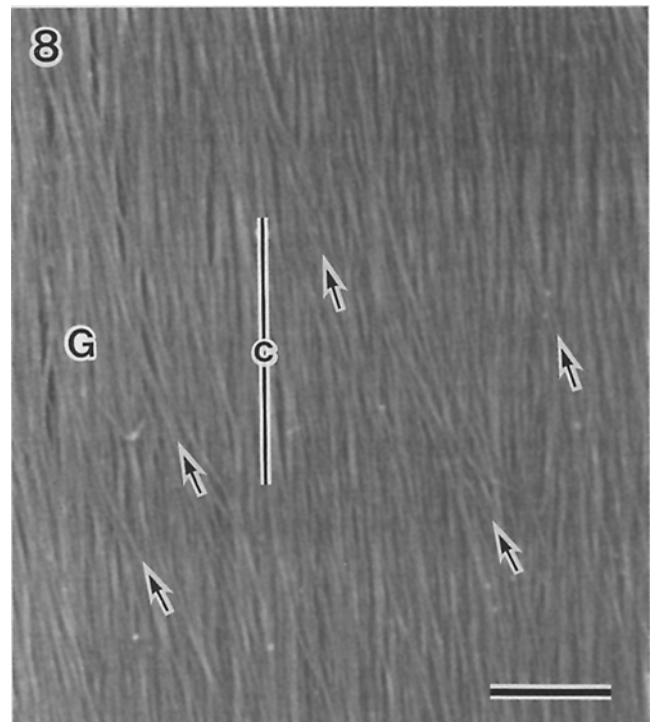


**Fig. 8.** Micrograph (FE-SEM) showing the counterclockwise rotation of MFs (arrows) oriented at an angle of about  $15\text{--}20^\circ$  to the fibre axis in a Z-helix over the MFs (c) that were deposited previously and oriented parallel to the fibre axis. G, gelatinous layer. Bar =  $0.5\ \mu\text{m}$

**Figs. 3–7.** Micrographs (FE-SEM) showing the progressive changes in orientation of MFs, with clockwise rotation (viewed from the lumen side), during formation of the G-layer in tension-wood fibres of Japanese ash

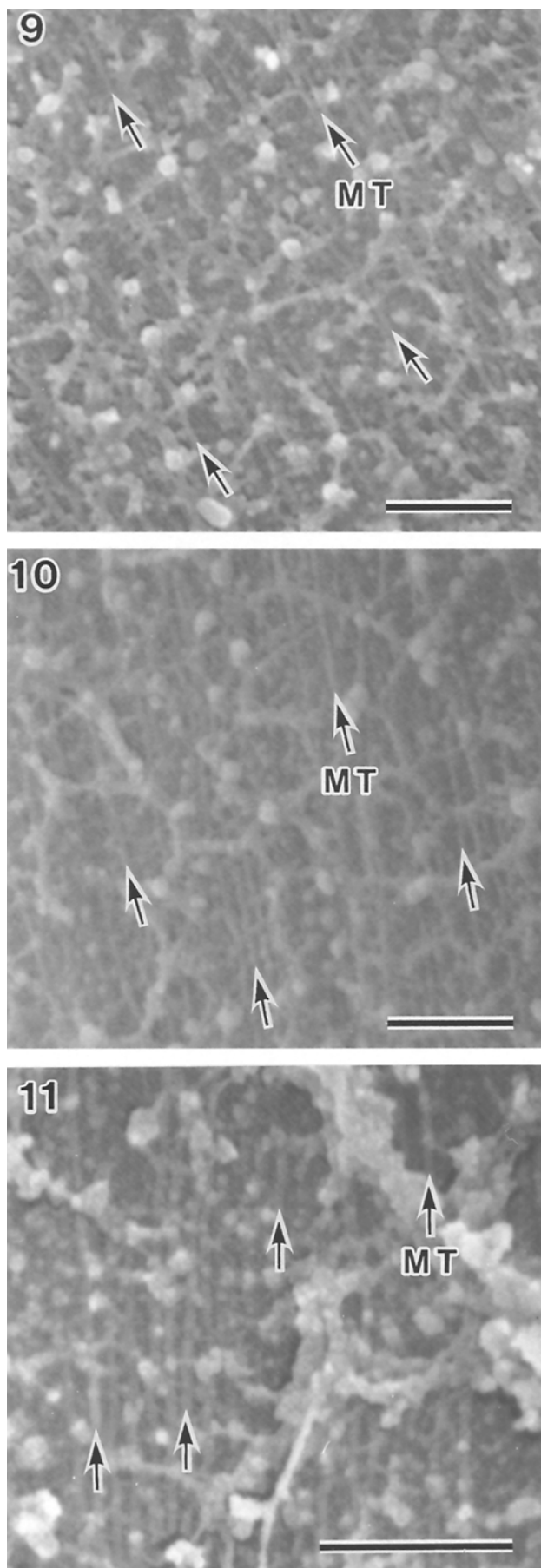
**Fig. 3.** The newly deposited MFs (arrows) are oriented at an angle of about  $30^\circ$  to the fibre axis in a steep Z-helix over the MFs (a) that were deposited previously at an angle of about  $35\text{--}40^\circ$  to the fibre axis in a Z-helix. GI, initiation of the gelatinous layer. Bar =  $1\ \mu\text{m}$

**Fig. 4.** The orientation of MFs (arrows) is similar to that of the newly deposited MFs in Fig. 3. Note that the MFs show a high degree of parallelism, suggesting the initiation of deposition of the G-layer. G, gelatinous layer. Bar =  $1\ \mu\text{m}$

**Fig. 5.** The newly deposited MFs (arrows) are oriented at an angle of about  $15^\circ$  to the fibre axis in a steep Z-helix over the MFs (b) that were deposited previously at an angle of about  $30^\circ$  to the fibre axis in a steep Z-helix. G, gelatinous layer. Bar =  $1\ \mu\text{m}$

**Fig. 6.** The MFs (arrows) are oriented at an angle of about  $10^\circ$  to the fibre axis in a steep Z-helix. Note the high degree of parallelism among the MFs. G, gelatinous layer. Bar =  $1\ \mu\text{m}$

**Fig. 7.** The MFs (arrows) are oriented parallel to the fibre axis. Note the high degree of parallelism among the MFs. G, gelatinous layer. Bar =  $0.5\ \mu\text{m}$



The transmission electron micrograph shows that MTs were aligned nearly parallel to the longitudinal axis of the fibre during formation of the G-layer (Fig. 14). The MTs were seen to be oriented parallel to the MFs and were also observed to be oriented parallel to one another. The number of MTs counted on the TEM micrographs tended to be similar to that counted on FE-SEM micrographs.

### Discussion

As MFs were deposited, their orientation changed progressively from the  $S_1$  layer to the G-layer, as viewed from the lumen side. At the initiation of secondary wall thickening, in particular at the beginning of formation of the  $S_1$  layer, the MFs were deposited at an angle of about  $45^\circ$  to the fibre axis in an S-helical orientation. Subsequently, the orientation of newly deposited MFs changed progressively with clockwise rotation, until MFs were oriented parallel (at an angle of about  $0^\circ$ ) to the fibre axis (Fig. 15a). The 'arced' pattern in the fibre wall of tension-wood has been observed by TEM in our laboratory (data not shown). This type of cell wall architecture can be considered to represent a semi-helicoidal pattern and it is consistent with the general helicoidal model proposed by a number of investigators (Roland and Mosiniak 1983; Neville and Levy 1984, 1985; Satiat-Jeunemaitre 1986; Roland et al. 1987).

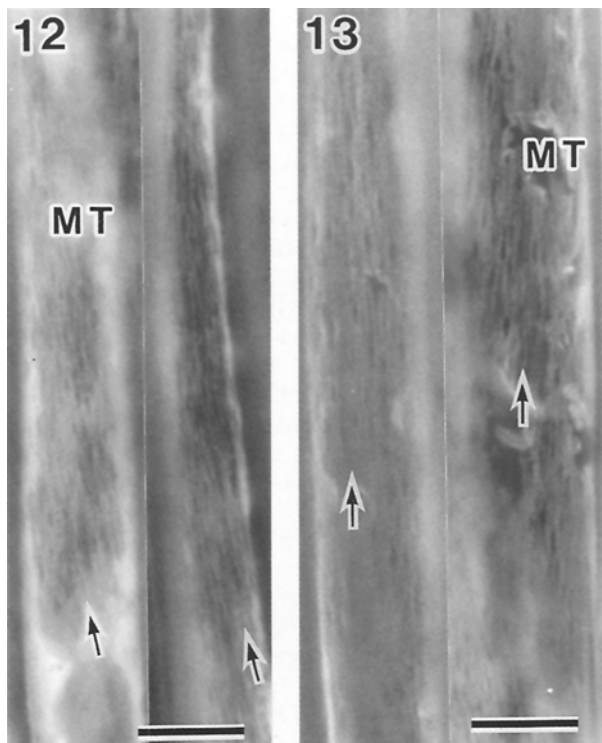
The gradual change in orientation of newly deposited MFs occurred at the outer region of the G-layer. The orientation of newly deposited MFs changed progressively, with clockwise rotation, until the MFs were oriented parallel to the fibre axis and then the rotation was arrested. At this stage, the repeated deposition of MFs occurred and a thick G-layer, with a consistent texture of parallel MFs, was formed. The present results support the hypothesis related to thickening of the cell wall (Roland and Mosiniak 1983; Roland et al. 1987; Abe et al. 1991). The details of the hypothesis are as follows: the orientation of MFs changes progressively in one direction with changing speed of rotation; when the rotation is arrested, a thick wall layer with a consistent texture is developed as a result of the repeated deposition of MFs. By contrast, the repeated alternation of rotational directions of MFs, responsible for deposition of a thick secondary wall layer reported by Kataoka et al. (1992) was not observed in the present investigation.

**Figs. 9–11.** Micrographs (FE-SEM) showing the progressive changes in orientation of MTs, with clockwise rotation (viewed from the lumen side), during formation of the G-layer in tension-wood fibres of Japanese ash

**Fig. 9.** The MTs (*arrows*) are oriented at an angle of about  $35\text{--}40^\circ$  to the fibre axis in a Z-helix at the beginning of formation of the G-layer. Note the high degree of parallelism among the MTs. *MT*, microtubule. Bar =  $0.5\ \mu\text{m}$

**Fig. 10.** The MTs (*arrows*) are oriented at an angle of about  $10^\circ$  to the fibre axis in a steep Z-helix. *MT*, microtubule. Bar =  $0.5\ \mu\text{m}$

**Fig. 11.** The MTs (*arrows*) are oriented parallel to the fibre axis. Note that the MTs are closely spaced with a high degree of parallelism. *MT*, microtubule. Bar =  $0.5\ \mu\text{m}$



**Figs. 12, 13.** Immunofluorescence micrographs showing the arrangement of MTs during formation of the G-layer in the developing tension-wood fibres of Japanese ash

**Fig. 12.** The MTs are arrayed obliquely (arrows) in a steep helical orientation to the fibre axis. *MT*, microtubule. Bar = 10 µm

**Fig 13.** The MTs are oriented parallel or nearly parallel (arrows) to the fibre axis. *MT*, microtubule. Bar = 10 µm

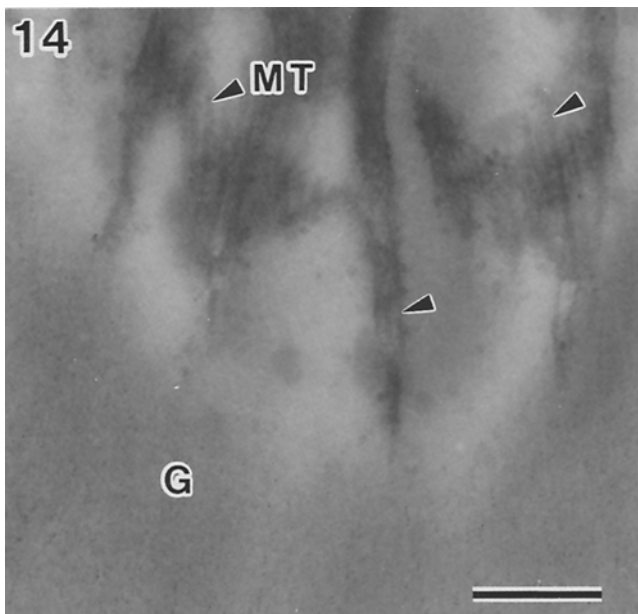


**Fig. 14.** Micrograph (TEM) of an obliquely cut section of a developing tension-wood fibre during formation of the G-layer. Note that the MTs (arrowheads) are aligned nearly parallel to the fibre axis and, are seen to be oriented parallel to one another. *G*, gelatinous layer; *MT*, microtubule. Bar = 0.5 µm

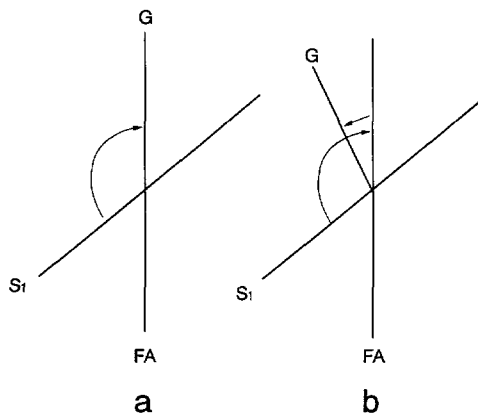


**Fig. 15a, b.** Diagrammatic representation of progressive changes in the orientation of MFs viewed from the lumen side, in two types of tension-wood fibre. **a** The clockwise rotation of MFs from the initiation of the  $S_1$  layer to the innermost surface of the G-layer for type-1 fibres. **b** The clockwise rotation and then the counterclockwise rotation of MFs from the initiation of the  $S_1$  layer to the innermost surface of G-layer at an angle of about  $25^\circ$  to the fibre axis in a steep Z-helix for type-2 fibres. *FA*, fibre axis

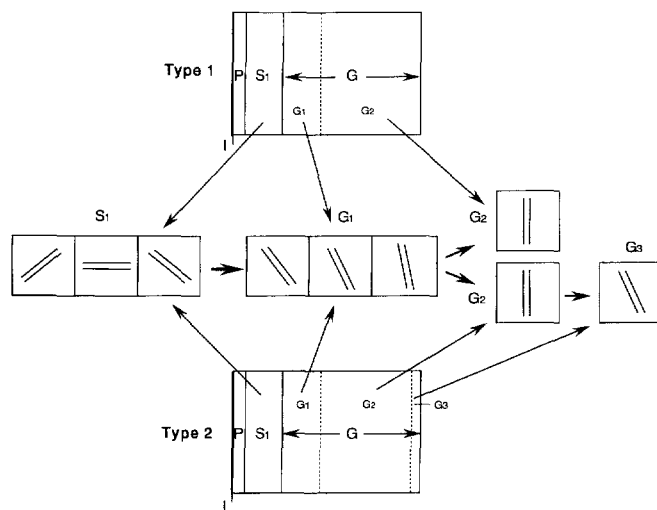


**Fig. 16.** A model of the orientation and deposition of MFs in the secondary wall of tension-wood fibres (type 1 and type 2) with the  $S_1 + G$  type of wall organization, viewed from the lumen side. *I*, intercellular layer; *P*, primary wall;  $S_1$ , outermost layer of the secondary wall; *G*, gelatinous layer;  $G_1$ , outer region of G-layer with progressive rotation of MFs;  $G_2$ , principal region of G-layer, with arresting of rotation, in which MFs are oriented parallel to the fibre axis;  $G_3$ , inner region of the G-layer, with the counterclockwise rotation of MFs

Two types of gelatinous fibre have been identified in the tension-wood of *Fraxinus mandshurica* var. *japonica*. In the first type, the rotation of MFs is arrested at an angle of about  $0^\circ$  to the fibre axis (Fig. 15a) and deposition eventually ceases after a desirable thickness has been achieved with a consistent texture of parallel MFs in the G-layer. In the second type, the mechanism of MF deposition is similar to that of the first type but the direction of rotation changes at a later stage of G-layer deposition. The orientation of the newly deposited MFs changes

progressively, with counterclockwise rotation, from parallel orientation (about 0° angle to the fibre axis) to an angle of about 25° to the fibre axis (Fig. 15b) with occasional arresting or cessation of rotation, which results in various degrees of deviation on the innermost surface of the G-layer. The resulting variation in angle among the fibres ranges from 5° to 25°, relative to the fibre axis with a Z-helical orientation. Observation from our laboratory shows such variation in the orientation of MFs on the innermost surface of the G-layer for the first time (data not shown). Our extensive investigations provide a clear understanding of the mechanism of this variation: the counterclockwise rotation of MFs from the parallel orientation (about 0° angle to the fibre axis) at the later stage of G-layer deposition (Fig. 15b) is responsible for such variation. The simultaneous presence of two types of gelatinous fibre in tension-wood has not previously been reported.

No MFs with an S-helical orientation were observed in the G-layer. Thus, the progressive changes in orientation of MFs in the secondary walls of tension-wood fibres from the initiation up to the final stage of deposition are clearly defined. On the basis of the present results, we now propose a model for the orientation and deposition of MFs in the secondary walls of tension-wood fibres with the S<sub>1</sub> + G type of wall organization (Fig. 16).

It has been reported that the orientation of MTs parallels the orientation of newly deposited MFs (Ledbetter and Porter 1963; Cronshaw 1965; Hepler and Palevitz 1974; Palevitz and Hepler 1976; Gunning and Hardham 1982; Giddings and Staehelin 1991; Seagull 1992; Abe et al. 1994). The present study showed that the MTs at the initiation of G-layer formation were oriented at an angle of about 35–40° to the fibre axis in a Z-helix and, thereafter, their orientation changed gradually with clockwise rotation until they were parallel to the fibre axis (Figs. 9–11). This change in orientation was similar to that of the MFs in the outer region of the G-layer (Figs. 3–7). The immunofluorescence micrographs revealed the orientation of MTs, which were obliquely arrayed, parallel or nearly parallel to the fibre axis, during deposition of the G-layer, corresponding to the results stated above. The TEM micrograph revealed the MTs oriented parallel to the fibre axis during G-layer formation. Thus, the present results indicate a close relationship between the orientation of MTs and that of MFs during formation of the G-layer. Similar observations by TEM have been reported in the differentiating tension-wood fibres of *Populus euramericana* Guinier (Nobuchi and Fujita 1972; Fujita et al. 1974) and of *Salix fragilis* L. (Robards and Kidwai 1972).

On the other hand, it has been stated that the orientation of MTs is not sufficient to explain the microfibrillar orientation in helicoidal walls (Neville and Levy 1984, 1985; Vian and Reis 1991; Emons et al. 1992). Concerning the mechanism of helicoid formation, it has been reported that the rotative changes of MFs in helicoidal walls are derived from a self-assembly process which resembles that of cholesteric liquid crystals (Neville and Levy 1984, 1985; Roland et al. 1987). However, our present results show strong evidence that microtubular orientation is related to the ordered orientation and deposition of MFs in the semi-helicoidal wall of the tension-wood fibre.

A recently proposed hypothesis suggests that MTs with a high density regulate the orientation of nascent MFs and those with a low density do not do so in the coenocytic green alga, *Chaetomorpha moniligera* Kjellman, (Kimura and Mizuta 1994). In their study, Kimura and Mizuta (1994) observed that MTs were oriented parallel to the longitudinally deposited MFs (the average density of MTs was 216 per 50 µm of wall) and were never oriented parallel to the transversely deposited MFs (the average density of MTs was 170 per 50 µm of wall). The density of MTs is generally higher in woody plants, in particular during the formation of secondary walls in tracheids or fibres. Abe et al. (1994) found 5–9 MTs per µm of wall in the tracheids of conifers, whereas Fujita et al. (1974) found approximately 20 MTs per µm of wall in the tension-wood fibres of *P. euramericana*. We also observed a high density of MTs in *F. mandshurica* var. *japonica* in the present investigation (17–18 MTs per µm of wall). Thus, it can be concluded that MTs with a high density play a significant role in regulating the orientation of newly deposited MFs in the secondary walls of wood fibres. The density of MTs and the extent of their parallelism are very high in tension-wood fibres during formation of the G-layer. On the other hand, a high degree of parallelism among MFs in the G-layer is evident. Therefore, it can also be concluded that the high degree of parallelism among MFs is closely related to the parallelism of MTs that are present at a high density.

We thank Dr. Y. Akibayashi, Mr. Y. Sano and Mr. T. Itoh of the Faculty of Agriculture, Hokkaido University, for their experimental or technical assistance.

## References

- Abe, H., Ohtani, J., Fukazawa, K. (1991) FE-SEM observations on the microfibrillar orientation in the secondary wall of tracheids. *Int. Assoc. Wood Anat. Bull.* n.s. **12**, 431–438
- Abe, H., Ohtani, J., Fukazawa, K. (1992) Microfibrillar orientation of the innermost surface of conifer tracheid walls. *Int. Assoc. Wood Anat. Bull.* n.s. **13**, 411–417
- Abe, H., Ohtani, J., Fukazawa, K. (1994) A scanning electron microscopic study of changes in microtubule distributions during secondary wall formation in tracheids. *Int. Assoc. Wood Anat. J.* **15**, 185–189
- Côté, W.A. Jr., Day, A.C. (1965) Anatomy and ultrastructure of reaction wood. In: *Cellular ultrastructure of woody plants*, pp. 99–124, Côté, W.A. Jr., ed. Syracuse Univ. Press, Syracuse
- Côté, W.A. Jr., Day, A.C., Timell, T.E. (1969) A contribution to the ultrastructure of tension wood fibers. *Wood Sci. Technol.* **3**, 257–271
- Cronshaw, J. (1965) Cytoplasmic fine structure and cell wall development in differentiating xylem elements. In: *Cellular ultrastructure of woody plants*, pp. 99–124, Côté, W.A. Jr., ed. Syracuse Univ. Press, Syracuse
- Dunning, C.E. (1968) Cell-wall morphology of longleaf pine latewood. *Wood Sci.* **1**, 65–76
- Dunning, C.E. (1969) The structure of longleaf pine latewood. I. Cell-wall morphology and the effect of alkaline extraction. *Tappi* **52**, 1326–1335
- Emons, A.M.C., Derksen, J., Sassen, M.M.A. (1992) Do microtubules orient plant cell wall microfibrils? *Physiol. Plant.* **84**, 486–493
- Fujita, M., Saiki, H., Harada, H. (1974) Electron microscopy of microtubules and cellulose microfibrils in secondary wall



- formation of poplar tension wood fibers. *Mokuzai Gakkaishi* **20**, 147–156
- Giddings, T.H. Jr., Staehelin, L.A. (1991) Microtubule-mediated control of microfibril deposition: a re-examination of the hypothesis. In: *The cytoskeletal basis of plant growth and form*, pp. 85–99, Lloyd, C.W. ed. Academic Press, London
- Gunning, B.E.S., Hardham, A.R. (1982) Microtubules. *Annu. Rev. Plant Physiol.* **33**, 651–698
- Harada, H., Côté, W.A. Jr. (1985) Structure of wood. In: *Biosynthesis and biodegradation of wood components*, pp. 1–42, Higuchi, T., ed. Academic Press, Orlando
- Harada, H., Miyazaki, Y., Wakashima, T. (1958) Electronmicroscopic investigation on the cell wall structure of wood. *Bull. Forest Exp. Sta.* **104**, 1–115
- Hepler, P.K., Palevitz, B.A. (1974) Microtubules and microfilaments. *Annu. Rev. Plant Physiol.* **25**, 309–362
- Hirakawa, Y. (1984) A SEM observation of microtubules in xylem cells forming secondary walls of trees. *Res. Bull. College Exp. For., Hokkaido Univ., Japan* **41**, 535–550
- Inomata, F., Takabe, K., Saiki, H. (1992) Cell wall formation of conifer tracheid as revealed by rapid-freeze and substitution method. *J. Electron Microsc.* **41**, 369–374
- Iwata, K., Hogetsu, T. (1988) Arrangement of cortical microtubules in *Avena* coleoptiles and mesocotyls and *Pisum* epicotyls. *Plant Cell Physiol.* **29**, 807–815
- Kang, K.D., Itoh, T., Soh, W.Y. (1993) Arrangement of cortical microtubules in elongating epicotyl of *Aesculus turbinata* Blume. *Holzforchung* **47**, 9–18
- Kataoka, Y., Saiki, H., Fujita, M. (1992) Arrangement and superimposition of cellulose microfibrils in the secondary walls of coniferous tracheids. *Mokuzai Gakkaishi* **38**, 327–335
- Kimura, S., Mizuta, S. (1994) Role of the microtubule cytoskeleton in alternating changes in cellulose-microfibril orientation in the coenocytic green alga, *Chaetomorpha moniligera*. *Planta* **193**, 21–31
- Ledbetter, M.C., Porter, K.R. (1963) A “microtubule” in plant cell fine structure. *J. Cell Biol.* **19**, 239–250
- Mia, A.J. (1968) Organization of tension wood fibers with special reference to the gelatinous layer in *Populus tremuloides* Michx. *Wood Sci.* **1**, 105–115
- Mueller, S.C., Brown, R.M. Jr. (1982) The control of cellulose microfibril deposition in the cell wall of higher plants II. Freeze-fracture microfibril patterns in maize seedling tissues following experimental alteration with colchicine and ethylene. *Planta* **154**, 501–515
- Neville, A.C., Levy, S. (1984) Helicoidal orientation of cellulose microfibrils in *Nitella opaca* internode cells: ultrastructure and computed theoretical effects of strain reorientation during wall growth. *Planta* **162**, 370–384
- Neville, A.C., Levy, S. (1985) The helicoidal concept in plant cell wall ultrastructure and morphogenesis. In: *Biochemistry of plant cell walls*, pp. 99–124, Brett, C.T., Hillman, J.R., eds. Cambridge University Press, Cambridge
- Nobuchi, T., Fujita, M. (1972) Cytological structure of differentiating tension wood fibres of *Populus euroamericana*. *Mokuzai Gakkaishi* **18**, 137–144
- Norberg, P.H., Meier, H. (1966) Physical and chemical properties of the gelatinous layer in tension wood fibers of aspen (*Populus tremula* L.). *Holzforchung* **20**, 174–178
- Palevitz, B.A., Hepler, P.K. (1976) Cellulose microfibril orientation and cell shaping in developing guard cells of *Allium*: the role of microtubules and ion accumulation. *Planta* **132**, 71–93
- Parameswaran, N., Liese, W. (1982) Ultrastructural localization of wall components in wood cells. *Holz als Roh- und Werkstoff* **40**, 145–155
- Robards, A.W., Kidwai, P. (1972) Microtubules and microfibrils in xylem fibres during secondary cell wall formation. *Cytobiologie* **6**, 1–21
- Roberts, I.N., Lloyd, C.W., Roberts, K. (1985) Ethylene-induced microtubule reorientations: mediation by helical arrays. *Planta* **164**, 439–447
- Roland, J.C., Mosiniak, M. (1983) On the twisting pattern, texture and layering of the secondary cell walls of lime wood. Proposal of an unifying model. *Int. Assoc. Wood Anat. Bull. n.s.* **4**, 15–26
- Roland, J.C., Reis, D., Vian, B., Satiat-Jeunemaitre, B., Mosiniak, M. (1987) Morphogenesis of plant cell walls at the supramolecular level: internal geometry and versatility of helicoidal expression. *Protoplasma* **140**, 75–91
- Satiat-Jeunemaitre, B. (1986) Cell wall morphogenesis and structure in tropical tension wood. *Int. Assoc. Wood Anat. Bull. n.s.* **7**, 155–164
- Scurfield, G. (1973) Reaction wood: its structure and function. *Science* **179**, 647–655
- Seagull, R.W. (1992) A quantitative electron microscopic study of changes in microtubule arrays and wall microfibril orientation during in vitro cotton fiber development. *J. Cell Sci.* **101**, 561–577
- Vian, B., Reis, D. (1991) Relationship of cellulose and other cell wall components: supramolecular organization. In: *Biosynthesis and biodegradation of cellulose*, pp. 25–50, Weimer, P.J., Haigler, C.H., eds. Marcel Dekker, Inc., New York